POLYTECHNICA UNIVERSITY OF BUCHAREST

FACULTY OF MATERIALS SCIENCE AND ENGINEERING

PhD THESIS

Development of new hybrid nanomaterials based on 3D graphene and TiO_2 for the degradation of dyes in industrial waters

Author : Elena Mădălina MIHAI (Mocirlă)

Scientific coordinator: Prof. Dr. Ing. Alexandra BANU

Evaluation board of the PhD Thesis

President	**Prof.dr.eng. Cristian PREDESCU** Politehnica University of Bucharest
Scientific coordinator	**Prof.dr.eng. Alexandra BANU** Politehnica University of Bucharest
Scientific referees	**Prof.dr.chem. Ecaterina MATEI** Politehnica University of Bucharest
	Dr.chem. Lucia Monica VECA INCD for Microtechnology IMT - Bucharest
	Prof.dr.eng. Alina-Adriana MINEA

Bucharest, 2023

Keywords: 3D graphene-titanium dioxide hybrid, Photocatalyst on substrate, RF-Sputtering, Sol-gel, Photocatalytic activity in the visible, Methyl orange

A current problem of the 21st century is pollution and especially water pollution. High content of persistent organic pollutants comes from textile finishing processes. A problem that persists is the removal of dyes from wastewater generated by large textile industries. The design and development of nanomaterials to be used in advanced oxidation processes have become of real interest to the field of materials engineering. The objective of the thesis is the synthesis, characterization, and testing of two 3D nanomaterials based on graphene and TiO_2 in order to obtain a high degradation efficiency under UV radiation and sunlight radiation. At the same time, in order to select the nanomaterial with the best degradation efficiency, two synthesis methods of titanium dioxide were considered, namely: Nanomaterials obtained by the sol-gel method denoted TiO_2^{SG}/3D-GF/Ni which present the pure anatase phase and the nanomaterials obtained by the RF Sputtering method denoted TiO_2^{RF}/3D-GF/Ni which present a combination of rutile anatase phases, with the predominant rutile phase.

After 180 minutes of UV exposure, the TiO_2^{SG}/3D-GF/Ni hybrid nanomaterial recorded the highest degradation efficiency of 99%, and the TiO_2^{RF}/3D-GF/Ni nanomaterial a degradation efficiency of 97.3% and only 89, 2 % in the case of 3D-GF/Ni.

In the case of exposure to the solar simulator, the degradation efficiency of the methyl orange dye after only 90 minutes for TiO_2^{SG}/3D-GF/Ni and TiO_2^{RF}/3D-GF/Ni was 99.5% and 97.5%, respectively.

Repeatability tests performed to evaluate the stability of TiO_2^{SG}/3D-GF/Ni and TiO_2^{RF}/3D-GF/Ni photocatalysts showed bright and stable photocatalysts that allow 3 sequential cycles of dye degradation with the same degradation efficiency after the third cycle.

Content

Introduction

A current problem of the 21st century is pollution and especially water pollution. High content of persistent organic pollutants comes from textile finishing processes. A problem that persists is the removal of dyes from wastewater generated by large textile industries.

Conventional purification methods, such as filtration, flocculation, coagulation, biological treatment, catalytic oxidation, adsorption on activated carbon, and chemical treatment using chlorine, potassium permanganate, ozone, hydrogen peroxide, and UV illumination, only transform persistent organic pollutants into waste.

An alternative to these methods is the advanced oxidation processes that have begun to be closely studied in order to obtain materials that help to oxidize dyes from water.

The design and development of nanomaterials to be used in advanced oxidation processes have become of real interest to the field of materials engineering.

The scientific research aims to obtain new materials for the optimization of photocatalysis processes by conferring a high efficiency, the reusability of the materials, and their long time of use.

Nanotechnology has a large impact on many scientific and technical fields, including environmental safety through various nanomaterials that use adsorption and separation processes, as well as a variety of other approaches, to remove pollutants, pathogens, and other hazardous elements.

Due to their high specific surface areas, micro interface properties, and remedial potential, nanomaterials have emerged as a topic of interest in environmental research.Different types of nanomaterials, generally powders, have been employed to treat wastewater from the textile industry. But these nanomaterials show a series of limitations, such as recovery after the photocatalysis process and/or deployment under UV/solar illumination for an improvement in degradation efficiency.

To this end, the current study aims to develop three-dimensional nanomaterials based on graphene and titanium dioxide, which increase the dye degradation efficiency in wastewater, both under UV radiation and sunlight.

3D graphene was grown on Ni foam by the chemical vapor deposition method using methane (CH4) as the carbon source, at a temperature of 1000°C and atmospheric pressure. The Ni foam on which graphene was grown has the advantage of obtaining a 3D structure with good mechanical stability that can be easily handled and even reused in photodegradation processes. Different methods, such as sol-gel, hydrothermal, and physical/chemical vapor deposition, enable the synthesis of titanium dioxide in the form of powders/nanoparticles, nanotubes, or thin films.

In this study, TiO_2 was synthesized by two different approaches, top-down and bottom-up, to find the most efficient, fastest, and cheapest method.

Although TiO_2 nanoparticles are among the most efficient photocatalysts, it presents a major disadvantage in the impossibility of total recovery after the photocatalysis process.

To overcome this limitation, herein thin TiO_2 films were deposited on the 3D/GF-Ni structure, in order to prepare stable, self-sustained, and reusable materials for the heterogeneous photocatalysis process. Several factors, such as graphene networks, the TiO2 synthesis method, the number of coatings, and the calcination temperature were found to influence the photocatalytic activity of the nanomaterial.

To select the nanomaterial with the best degradation efficiency, two methods were considered for the synthesis of titanium dioxide, namely: the sol-gel method, for the preparation of TiO_2^{SG}/3D-GF/Ni nanomaterials which showed the pure TiO_2 anatase phase, and the RF Sputtering method for the preparation of TiO_2^{RF}/3D-GF/Ni nanomaterials that exhibited a combination of TiO2 rutile and anatase phases, with rutile as the predominant phase.

To establish the optimal thermal treatment for the anatase phase synthesis, different depositions were performed on the FTO substrate, and the calcination time and temperature parameters were varied.

The chemical, morphological, and structural characteristics, as well as the photocatalytic properties of the developed nanomaterials, were highlighted through specific analyzes and laboratory tests.

Therefore, the morphological-structural characteristics and composition of the obtained nanomaterials were analyzed using scanning electron microscopy (SEM), X-ray diffraction (XRD), and Raman spectroscopy. In addition to the specific materials engineering characterization, the PhD thesis also addresses wastewater treatment methods, such as adsorption and photocatalysis.

The thesis is structured in two parts and 5 chapters comprising 17 tables, 56 figures, and 225 bibliographic references.

The first part includes two chapters, Chapter 1 entitled "*The current stage of research in the field of obtaining 3D nanomaterials with photocatalytic properties*" consists of general literature information regarding various types of nanomaterials and their photocatalytic properties, with an emphasis on graphene and TiO_2-based nanostructures and their possible applications in photodegradation processes.

Chapter 2 entitled "Objectives, research methods, and equipment " includes information on the objectives, the methodology of the research, and the experimental design. Additionally, this chapter briefly describes the analysis methods and equipment used to characterize the nanomaterials obtained based on 3D graphene and TiO_2.

The second part, experimental studies and original contributions, is structured into three chapters whose brief content is as follows: Chapter 3 entitled "Studies on the synthesis and characterization of 3D graphene-titanium dioxide hybrid nanomaterials" presents the synthesis approach and characterization of each photocatalytic material, 3D graphene, and TiO2-graphene hybrids. The characterization of the obtained nanomaterials was carried out by performing tests regarding the structure and morphology, using X-ray diffraction measurements (XRD), Raman spectroscopy, and scanning electron microscopy (SEM). To

understand the photocatalytic activity under different irradiation sources, diffuse reflectance measurements were performed to evaluate the band gap of titanium dioxide.

Chapter 4, entitled "Studies regarding the evaluation of the photocatalytic performances of 3D graphene and TiO_2-based nanomaterials. Case study – photodegradation of methyl orange " Reveals the photocatalytic performances of 3D-GF/Ni and TiO_2/3D-GF/Ni hybrids on methyl orange (MO) dye degradation.

To demonstrate the degradation efficiency of the studied dye, the photocatalysis tests were performed in the presence of both UV lights (365 nm) and sunlight.

In addition, the obtained 3D nanomaterials were tested for reusability and found an efficiency of approximately the same value in the third cycle.

Chapter 5 entitled "Conclusions, original contributions, and perspectives" synthesizes the conclusions of the research highlighting the original contributions and the future directions of the research. Therefore, two nanomaterial hybrids based on 3D graphene and TiO_2 were designed, prepared, and tested. The hybrids, TiO_2^{SG}/3D-GF/Ni and TiO_2^{RF}/3D- GF/Ni were obtained by two different methods: the sol-gel and the RF Sputtering, respectively.

The nanomaterials that have been synthesized and characterized, have the advantage of immobilizing titanium dioxide on a fixed support, which makes them simple, low-cost, reusable, and efficient photocatalysts.

Both nanomaterials showed a response in the visible range, recording a significant dye degradation efficiency.

PART I. LITERATURE REVIEW, OBJECTIVES OF THE THESIS

Chapter 1

The current state of research in the field of obtaining 3D nanomaterials with photocatalytic properties

1.1 General considerations

As the human population and environmental degradation continue to grow, the lack of a source of potable water is a big concern given the current state of the world's water resources. Drinking water shortages are expected to worsen in the coming years, with water shortages occurring globally due to droughts, population growth and urbanization. The textile industry is one of the largest sources of water contamination with dyes. Numerous technologies, such as distillation, treatment with chemical disinfectants, sand filtration, porous membrane filtration, and advanced oxidation processes have been used to purify water. Unfortunately, these proved to be ineffective due to the large volume of wastewater. Contamination of waters with persistent organic pollutants prevents these technologists from completely removing them, resulting in toxic waste after the applied treatments. Wastewater treatment technologies

also require high maintenance costs. All these inconveniences led to the need to develop nanomaterials that present photocatalytic activity for dye removal processes from contaminated waters.

Nanomaterials are defined as materials consisting of nanoparticles of which at least 50% have one or more dimensions between 1 and 100 nm.[1] Their small sizes not only increase the bulk surface functionality, but also lead to physical properties that often differ from their macroscopic or bulk counterparts in many aspects, including electronic, optical, and magnetic characteristics. [2–7]

Environmental applications of nanotechnology include water and wastewater treatment, where various nanomaterials use adsorption and separation processes, as well as a variety of other approaches, such as heterogeneous photocatalysis in the presence of semiconducting nanomaterials, to remove pollutants, pathogens, and other hazardous elements.

Dyes are natural or synthetic organic substances, which have the property of coloring bodies with which come into contact, textile fibers, leather, paper, etc., and which absorb light from the visible range of the electromagnetic spectrum. They are classified according to their chemical structure and their properties towards fibers in the dyeing process. The chemical structure of the dyes classifies them into two categories according to the nature of the structural units and according to the nature of the typical chromophores.

Depending upon their chemical structure, the dyes are structured as follows: azo (e.g., methyl orange), nitro, nitroso, methine and polymethine, anthraquinone, acridine, azine (methylene blue), indigo dyes, sulfur dyes, etc. [9].

1.2 Materials with photocatalytic properties used in advanced wastewater treatment

Materials engineering in heterogeneous photocatalysis is associated with the transformations that take place at the molecular level on the catalyst surface. Photocatalyst efficiency is correlated with their specific surface area. In this context, powder nanostructures with a high specific surface area were synthesized, but it is difficult to recover after water treatment unless immobilized on a substrate. Moreover, the efficiency is further improved if the substrate is sufficiently conductive to favor the separation of the electron-hole pairs generated upon interaction with the light source [23,24].

Characteristics of titanium dioxide

Titanium dioxide is an n-type semiconductor that absorbs photons in the UVA range (320 - 400 nm), which limits its application in systems using solar energy; however, TiO_2-based photocatalytic systems are frequently used in multiple applications as an electrode in photo(electro) chemical cells [27], capacitors or solar cells [28-31], photodegradation of organic compounds, or water and air purification in the presence of artificial UV sources.

An advantage of titanium dioxide is its low synthesis cost, as well as the chemical stability and high photocatalytic efficiency in its absorption range. Numerous studies presented various methods for the synthesis of titanium dioxide in all its polymorphic forms (anatase, rutile, and brookite), as well as their exceptional photocatalytic activity in the UV range. To shift the photocatalytic activity to the visible range several approaches were proposed to reduce the

band gap of TiO_2, namely metals or non-metals doping, reducing TiOx, and dyes sensitizations.

Characteristics of graphene

Graphene and, recently, 3D graphene is a relatively new material that plays a very important role in photocatalytic processes.

Graphene consists of sp2 hybridized carbon atoms with a hexagonal arrangement. Ever since it was discovered in 2004 [38], graphene and its derivatives have been used widely in many applications, photocatalytic nanocomposites being one of them. Graphene has a unique two-dimensional structure with high specific surface area, high conductivity, and electron mobility. Consequently, graphene can more effectively inhibit the recombination of electron-hole pairs generated upon interaction with the irradiation light, and, thus, improves the photocatalytic efficiency of the composite nanomaterials [39]. Graphene has a high thermal conductivity (≈ 5000 W m-1 K -1), excellent mobility of charge carriers at room temperature (200 000 cm2 V-1 s -1), a very high specific surface area (calculated ≈ 2630 m2 g -1), a high transparency, a very high mechanical strength (2.4 ± 0.4 TPa), and the capability to withstand high current densities (108 A cm-2) [40-45].

Characteristics of titanium dioxide-graphene hybrids

In the last decades, various attempts have been made to improve the catalytic efficiency of TiO_2 [58,59]. Due to its large band gap, TiO_2 is only active under UV light irradiation; Given that the percentage of UV light is less than 5% of the total incident solar spectrum on Earth, in recent years, research has focused on extending the light absorption of TiO_2 into the visible range. The goal of photocatalysis research in the presence of TiO2, as well as in the case of other semiconductors, is the efficient combination of TiO2 with other nanomaterials to achieve both the activation in the visible range and the improvement of the adsorption capacity, with the simultaneous reduction of the recombination rate of electron–hole pairs.

1.2.1 Synthesis methods

The sol-gel method used to deposit titanium dioxide thin films

TiO_2-based photocatalytic thin films and nanostructures are now widely used for a variety of applications such as environmental remediation, self-cleaning glass, hydrogen generation, and antibacterial material due to their chemical, electrical, and optical properties [89-94].

Thin films can be applied to various substrates and are used instead of powder materials, leading to substantial cost reductions for photocatalyst recovery and regeneration processes. Designing nanoscale thin films enables distinct surface functionalities with mechanical, chemical, and physical properties, and enhanced photocatalytic performance [95]. TiO_2 thin films with photocatalytic properties can contain anatase, rutile, or a combination of both phases.

TiO_2 thin films have been synthesized by several complex techniques, such as chemical vapor deposition (CVD) [96,97], hydrothermal synthesis [98,99], metal-organic chemical vapor deposition (MOCVD) [100,101], sputtering [102,103], liquid phase deposition (LPD) [104,105], electrophoretic deposition [106], physical vapor deposition (PVD) [107], pulsed laser ablation deposition [108,109], sol-gel [110,111], electrochemical deposition [112], atomic layer deposition (ALD) [113], etc. Most of these methods are carried-out at high temperatures and pressures, with the sol-gel method exception, a common and simple synthesis method due to its efficacy, compositional homogeneity, and reliability.

RF Sputtering method used to deposit TiO_2 thin films by a "top-down" approach has the advantage of working well with isolated targets and allowing large and uniform coverages of the surfaces. In addition, the electric field inside the plasma deposition chamber changes with the RF frequency, which circumvents any charging effects. During the magnetron sputtering, argon and oxygen are the plasma and reactive gases. Therefore, the oxygen partial pressure can influence the discharge parameters, such as plasma potential, discharge voltage, deposition rate, and ionic composition of the plasma and, hence, the composition and crystallinity of the deposited TiO2 films, essential properties in the photocatalytic processes.

Chemical vapor deposition for the graphene growth

There are a variety of CVD methods that can be employed for graphene-based materials synthesis. Depending on the characteristics of the processing parameters, these methods can be classified according to temperature, pressure, precursor nature, gas flow rate, activation/energy source, etc.

A series of precursors were reported for the graphene's growth processes, such as solid, liquid, and gaseous carbon sources. The most commonly used carbon precursor is in gaseous forms, such as methane. Generally, graphene deposition by CVD uses metal as a growing substrate and catalyst (eg Cu, Ni) in the presence of a gaseous mixture of hydrocarbons and hydrogen at high temperatures (1000 C in the case of nickel substrate) and atmospheric pressure. In addition to the catalytic role, the metallic substrate also plays the role of a template. In other words, it gives the final shape to the carbonaceous material. Thus, metallic films produce 2D graphene, while metallic foams yield 3D graphene networks.

Applications of graphene- and TiO_2-based nanomaterials in the degradation of methyl orange dye in wastewater

The aim of developing such TiO_2-graphene hybrids was to extend the photocatalytic activity to the visible range. Multiple studies demonstrated the potential of rGO-TiO2 composites in the photocatalytic processes. Composites' photoactivity in MO degradation demonstrated that different crystalline phases of TiO_2 exhibit various behavior under UV and visible light irradiation due to the distinct charge transfer mechanisms. Photocatalytic performances of composites based on graphene and its derivatives and titanium dioxide in MO degradation processes depend on their nature and composition. The efficiency of photocatalytic degradation under UV source has reached 70% [169] or even 100% [168, 170, 173], while the performances in the visible range, a much lower number of studies, ranging between 50% [170] and 99% [167].

Chapter 2

Objectives, methods of analysis, and equipment

2.1 Aim and objectives

The PhD thesis entitled "Development of new hybrid nanomaterials based on 3D graphene and TiO_2 for the degradation of dyes in industrial waters" has the purpose of designing, obtaining, characterizing, and optimizing three-dimensional nanomaterials based on graphene and titanium dioxide, with potential for the degradation dyes from wastewater from the textile industry.

The general objective of the studies undertaken in this PhD thesis was the synthesis and characterization of advanced nanomaterials with oxidative properties of persistent organic pollutants from wastewater. The main aspects/characteristics that were the foundation of the current studies are the synthesis of nanomaterials and the degradation efficiency recorded in the UV-Vis domain, with the emphasis on the visible range, good stability, and large active surface area to allow the possibility of recovering and reusing the synthesized photocatalysts, as well as a low cost for the synthesis of the material to enable a technological transfer to the industrial field. Starting from these cumulative requirements, the synthesis of a nanostructured hybrid nanomaterial consisting of three-dimensional graphene and titanium dioxide on a nickel substrate was proposed. A case study on the polluting dye methyl orange was conducted to underline the photocatalytic activity of the synthesized nanomaterials.

2.2 Development of the conceptual model of the research

To obtain nanomaterials with the role of photocatalyst, we started from the existing information in the specialized literature about the synthesis of accessible and durable nanomaterials that can present multiple uses in the decontamination of organic pollutants from wastewater.

The research methodology, the work plan, the synthesis, the morpho-structural characterization, and photocatalytic evaluation of the nanomaterials were carried out at the National Research and Development Institute for Microtechnology - IMT Bucharest. The 3D-GF/Ni material obtained by the CVD method was provided by the National Research and Development Institute for Electrical Engineering ICPE-CA. The electrochemical characterization of the nanomaterials was carried out in the corrosion and surface engineering laboratory of the Faculty of Industrial Engineering and Robotics.

The stages that formed the basis of the development of the doctoral thesis are the following:

I. Synthesis of materials

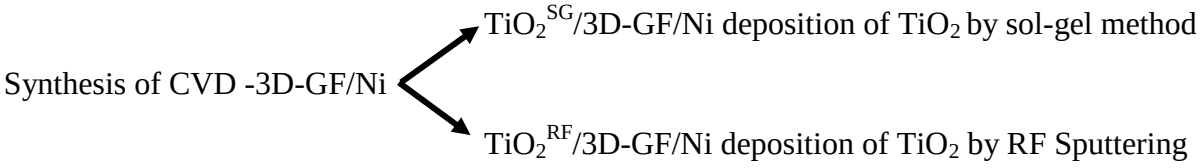

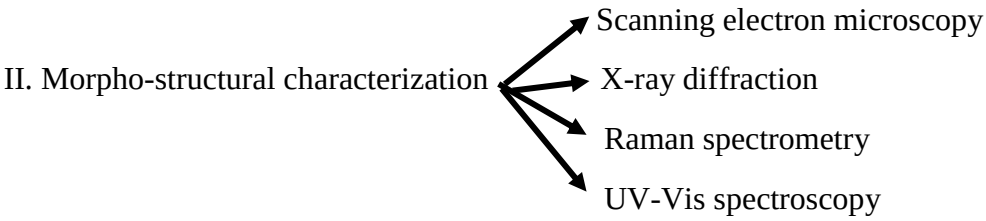

III. Testing the photocatalytic properties of the nanomaterial in the presence of MO dye and exposure to UV and Visible light.

PART II- EXPERIMENTAL STUDIES AND ORIGINAL CONTRIBUTIONS

Chapter 3

Studies on the synthesis and characterization of 3D graphene and titanium dioxide nanomaterials

This chapter presents the synthesis and characterization of 3D-GF/Ni, TiO_2^{SG}/3D-GF/Ni and TiO_2^{RF}/3D-GF/Ni nanomaterials.

3D-GF/Ni graphene networks were obtained by chemical vapor deposition (CVD) technique on standard commercial nickel foam using a mixture of methane and hydrogen in the presence of argon.

The methods used in this thesis to deposit TiO_2 thin films are the sol-gel, a “bottom-up” approach, and RF Sputtering, a "top-down" approach.

The first consisted of the TiO_2 sol synthesis, deposition on 3D-GF/Ni, and subsequent thermal treatment to yield the nanomaterial denoted TiO_2^{SG}/3D-GF /Ni. The latter is an RF sputtering deposition from a titanium target in an argon/oxygen gas mixture onto 3D-GF/Ni to yield the nanomaterials denoted TiO_2^{RF} /3D - GF/Ni.

The two methods enabled the synthesis of pure anatase phase, in the case of the sol-gel method, and the mixture of anatase and rutile phases, in the case of the RF sputtering method.

3.1.1 Synthesis of 3D graphene structures on Ni foam

The general synthesis method of 3D-GF/Ni is shown schematically in figure 3.1.

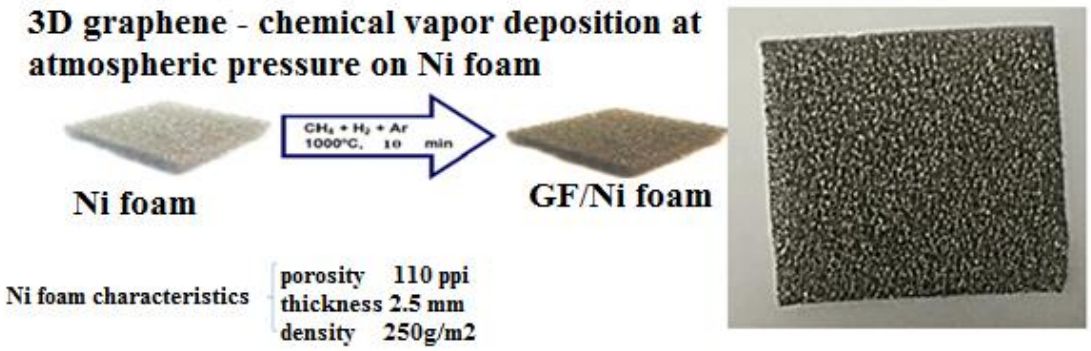

Fig. 3.1 Schematic representation of 3D-GF/Ni material synthesis by CVD and photo image of the material

In order to obtain the 3D graphene structure, a commercial nickel foam produced by Gelon LIB Group with the following characteristics was used as a template: number of pores per inch: 110 PPI, density ≥ 250 g/m2, thickness ≤ 2.5 mm.

The 3D graphene structure was synthesized by the chemical vapor deposition (CVD) method on a nickel foam at a temperature of 1000°C and atmospheric pressure, using methane (CH4) as a carbon source. The gases used in the CVD process were supplied by SIAD Romania and have the following characteristics: argon (purity > 99.999%), hydrogen (purity > 99.995%) and methane (purity > 99.9995%). Graphene was grown on nickel foam of 5 cm x 5 cm in size.

3.1.2 Morpho-structural characterization of the 3D-GF/Ni material

Scanning electron microscopy (SEM) examination of the synthesized materials reveals the formation of a continuous graphene network with specific wrinkles, which reproduces the structure of Ni foam. Subsequent structural characterizations indicate the formation of graphene with one and several layers, with an insignificant development of defects, regardless of the growing time, 10 or 15 minutes. The morphological aspect of the 3D-GF/Ni nanomaterials grown for 10 and 15 minutes are presented in figure 3.1.1, which shows a smooth graphene surface with a well-defined structure.

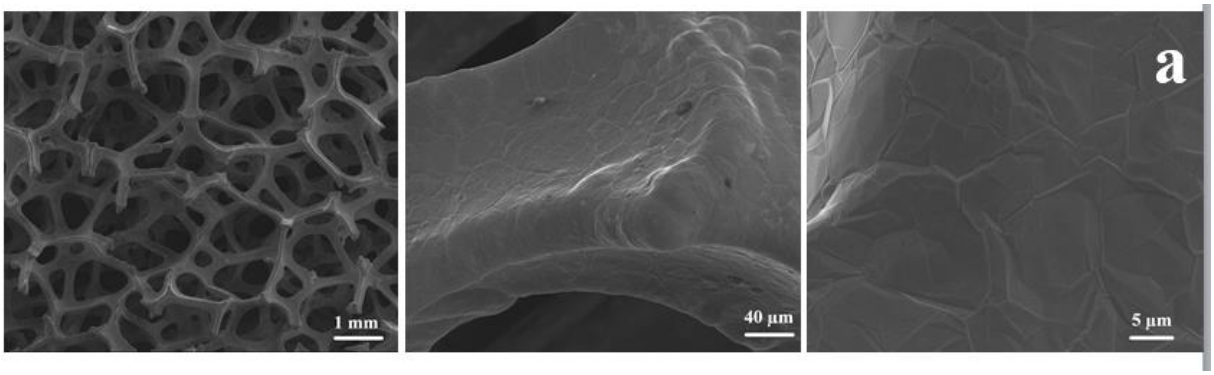

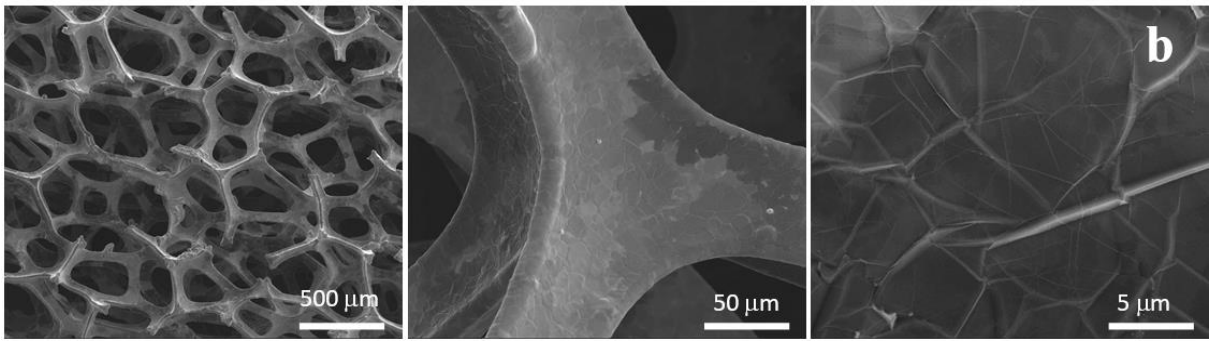

Fig 3.1.1 SEM images of nanomaterials a) 3D-GF10/Ni b) 3D-GF15/Ni

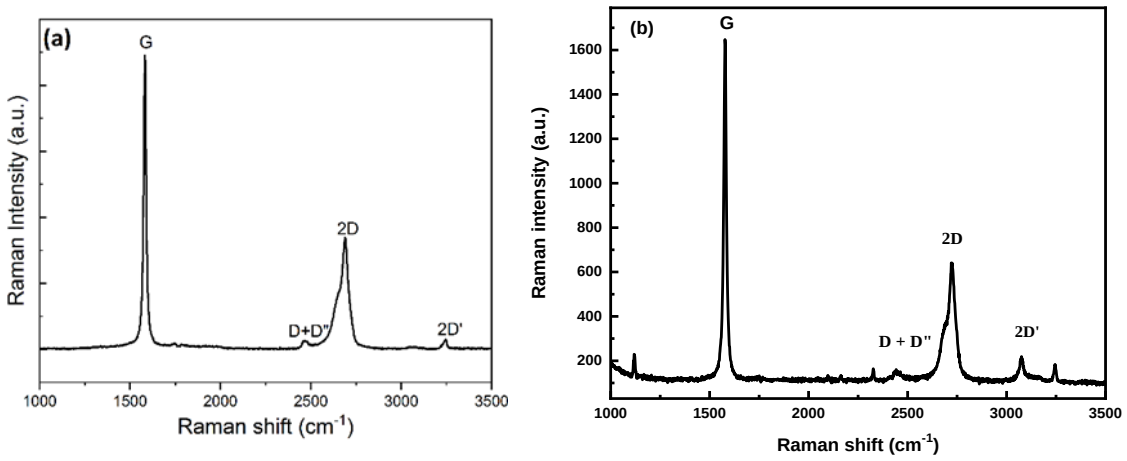

Fig 3.1.2 Raman spectra for a) 3D-GF10/Ni and b) 3D-GF15/Ni

Data recorded by Raman spectroscopy, shown in Fig. 3.1.2, indicate that the 10- and 15-min grown graphene layer (3D-GF/Ni) exhibits the characteristics of a high-quality sp2 material, free of defects such as growth discontinuities or other structural defects.

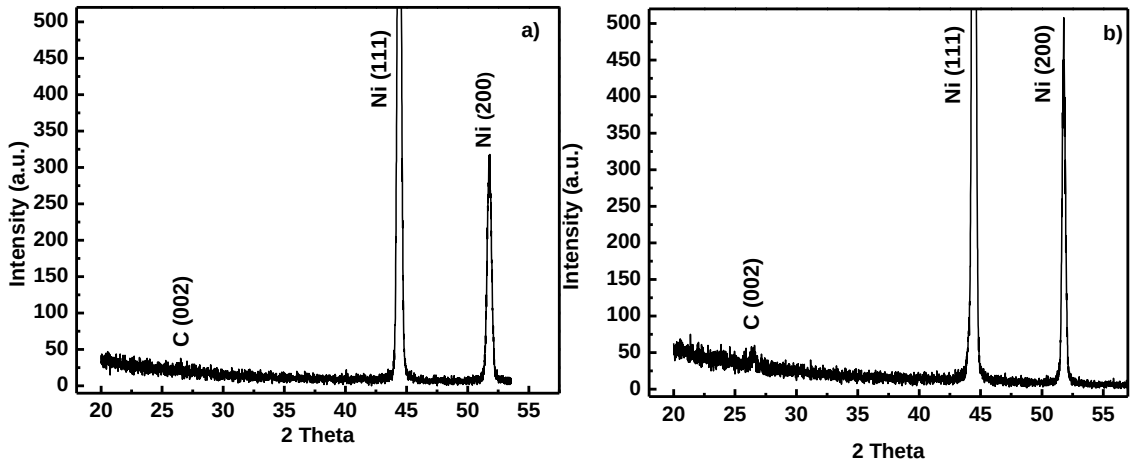

Fig. 3.1.3 X-ray diffractograms for a) 3D-GF10/Ni and b) 3D-GF15/Ni

The X-ray diffraction spectra of the 3D-GF10/Ni and 3D-GF15/Ni structures are shown in figure 3.1.3.

The diffraction peaks of the carbon lattice and the nickel substrate are distinguishable in both structures. The position of the graphite diffraction is at $2\theta = 26.44°$ for both samples.

In conclusion, the graphene growth time (10 or 15 minutes) does not influence the morphology or structure of the graphene network. All the characteristics of the materials presented in parallel are similar or even identical.

3.2.1 Synthesis of the anatase/graphene TiO_2^{SG}/3D-GF/Ni hybrid material

The synthesis of the sol was carried out in a glovebox under nitrogen from a solution of titanium (IV) isopropoxide (0.966 g) in ethanol (34 mL). After 5 min of stirring at 300 rpm, 0.5 mL of 37% HCl was added gradually, followed by additional stirring for 1 h at 60°C in a hermetically sealed glass vial and then left at room temperature for 24 hours before deposition.

The TiO_2 film was deposited on the three-dimensional graphene and calcined in the air at the optimal time and temperature for the anatase phase formation. The TiO_2 sol was dip-coated on both sides of the 3D-GF/Ni substrate using three or four dip cycles with a 10-min treatment at 100°C after each deposition cycle.

The substrate was then transferred to the furnace and calcined at 450°C in air for 2 h with a heating ramp of 3.5 degrees/min, followed by natural cooling to room temperature to produce the graphene-based TiO_2 hybrid, denoted as TiO_2^{SG}/3D-GF/Ni characterized and further used in the photocatalytic tests.

3.2.2 Morpho-structural characterization of the TiO_2^{SG}/3D-GF/Ni hybrid

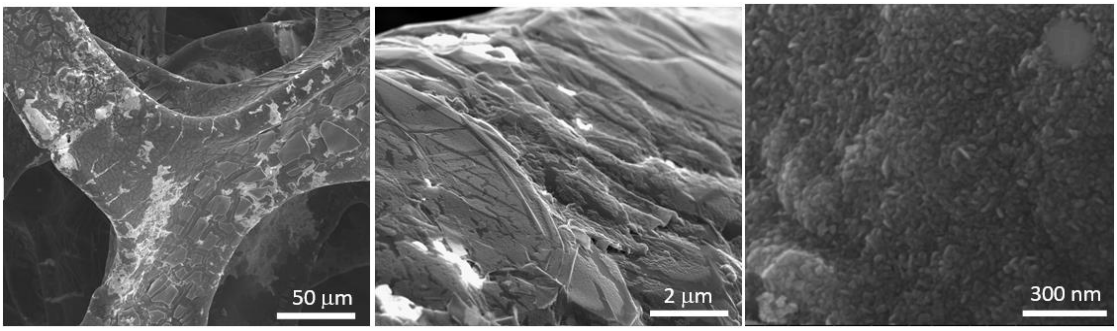

Fig. 3.2.1 SEM images of the TiO_2^{SG}/3D-GF/Ni nanomaterial at different magnifications, showing the uniformity and morphology of the TiO_2 film, which completely covers the 3D-GF/Ni structure with the formation of nanoflower-like nanostructures.

After deposition of the TiO_2 thin film and calcination at 450°C for 2 hours, the TiO_2 thin film follows the architecture of the 3D-GF/Ni foam and shows the formation of nanoflower-type nanostructures (Fig. 3.2.1). After 4 deposition cycles, the TiO_2 film uniformly covers the surface of the graphene foam with only a few cracks.

The structural characterization of the 3D-GF/Ni network coated with TiO_2 investigated by XRD and Raman analysis is presented in Fig. 3.2.2, and Fig. 3.2.3, respectively indicating the

presence of all components. The X-ray diffraction spectrum, presented in Fig 3.2.2, shows a graphite diffraction peak at 2θ = 26.44 along with peaks at 44.50°, 51.86°, and 63.39° corresponding to the Ni substrate, and the peaks assigned to (101), (200), (211), and (213) planes characteristic to the anatase phase.

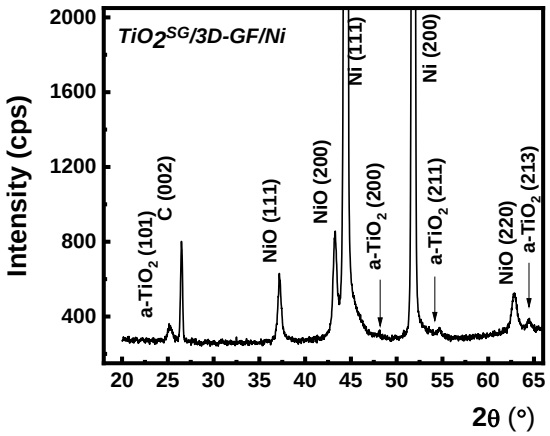

Fig. 3.2.2 X-ray diffractogram for the TiO_2^{SG}/3D-GF/Ni nanomaterial

The formation of the anatase phase was also unambiguously confirmed by the Raman analysis shown in Fig. 3.2.3 The fingerprints of the anatase phase with Raman active modes A1g+2B1g+3Eg centered at 147 (Eg), 198 (Eg), 398 (B1g), 517 (B1g or A1g), and 636 (Eg) cm-1, indicate towards the formation of the pure anatase phase. Furthermore, the absence of the D band, typically centered at ~1350 cm-1, associated with defects in the graphene layers, indicates the growth of the high-quality graphene networks.

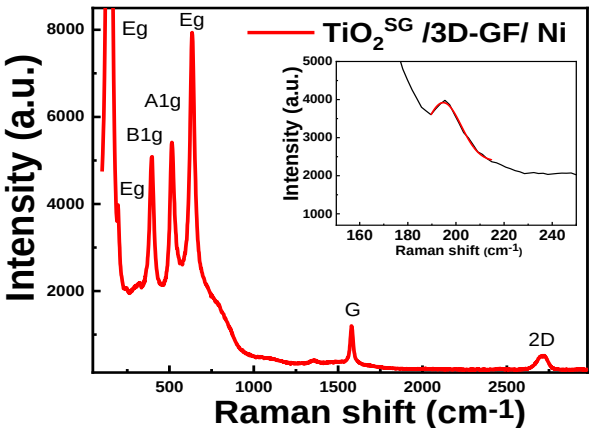

Fig. 3.2.3 Raman spectrum for the TiO_2^{SG}/3D-GF/Ni nanomaterial

Band gap measurements by Diffuse Reflectance Spectroscopy (DRS) enabled the estimation of the band gap at a value of 3.15 eV for the TiO_2 films deposited on the quartz substrate and 3.07 eV for the one deposited on the graphene surface after etching the nickel support (3D-

GF), results which are suggesting an insignificant influence of the graphene on the TiO_2 band gap.

Cyclic voltammetry curves are electrochemical tests that evaluate the redox potentials of the reversible system. The electrochemical tests were performed in a system consisting of the working sample, the Ag/AgCl/3M reference electrode and the Pt counter electrode, in Na_2SO_4 solution, at neutral pH and acid pH (3), at room temperature. The potential range is from -0.5 to 1V, the scan rate is 100 mV/s.

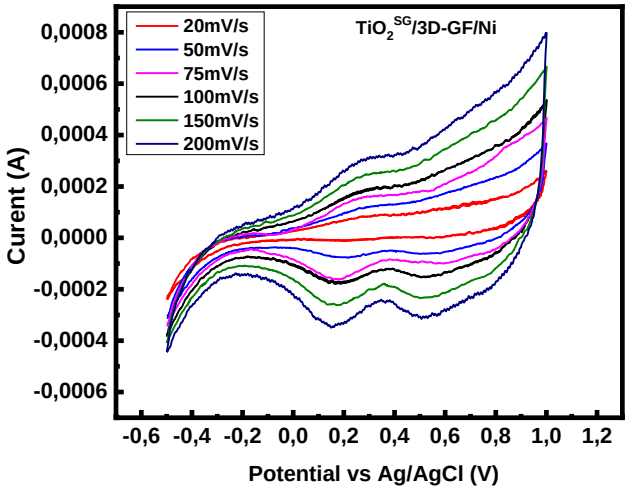

Fig. 3.2.4 TiO_2^{SG}/3D-GF/Ni cyclic voltammogram – Variation with the scan rate, in the potential range -0.5 - +1V, in a neutral medium

To verify the performance of the TiO_2^{SG}/3D-GF/Ni nanomaterial synthesized at 450^0C for 2h, CV tests were performed at different scan rates. As observed in Fig. 3.2.4, the shape of the CV curve is relatively constant with increasing the scanning rate in the -0.5 - 1 V range.

The CV curves maintain good quasi-reversibility with the larger integration area at the higher scanning rate, showing that the performance of the nanomaterial is relatively good with the variation of applied potential, and the nanomaterial holds significant capacitive properties.

The increase in current density is proportional to the increase in the scan rate, which can be explain by the fast diffusion and migration of ions in the closed system.

3.3 Studies regarding the synthesis and characterization of the TiO_2^{RF}/3D-GF/Ni hybrid nanomaterial

3.3.1 Synthesis of the TiO_2^{RF}/3D-GF/Ni hybrid material

In the second approach, the TiO_2 thin film was deposited using a Plasmalab 400 RF Sputtering System (Oxford Instruments, UK). The depositions were performed from a titanium (Ti) target (99.5%) in the presence of argon (Ar - 99.999%) as the sputtering gas and molecular oxygen (O2 - 99.999%) as the gas reactive. For these sets of depositions, the samples oscillated in a parallel plane under the Ti target with an angle of 30° (15° left and 15° right) for better uniformity of the film.

3.3.2 Characterization of the TiO_2^{RF}/3D-GF/Ni hybrid material

The TiO_2 thin film deposited by the RF Sputtering method with a thickness of 30 nm has a granular morphology, comprising aggregated and interconnected nanoparticles in a continuous and uniform film on the 3D-GF/Ni substrate (Fig. 3.3.1).

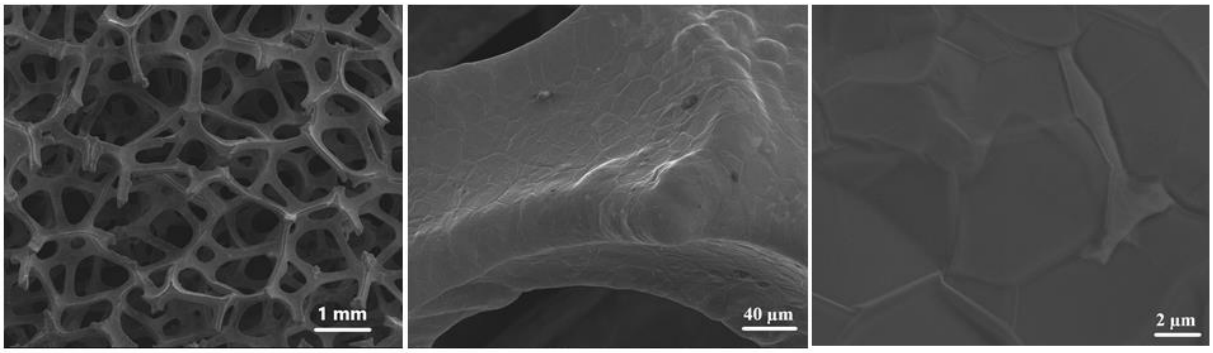

Fig 3.3.1 SEM images at different magnifications for the TiO2RF/3D-GF/Ni nanomaterial

The X-ray diffraction spectra of TiO_2^{RF}/3D –GF/Ni are shown in figure 3.3.2. The graphite diffraction peak is located at $2\theta = 26.44$ °, which leads to an interplanar spacing of ~ 0.36 nm before and after TiO_2 deposition, according to Bragg's law: $2d_{hkl}\sin\theta = \lambda$, where λ is the wavelength of incident X-ray. The XRD analysis, shown in Fig 3.3.2b, of the TiO_2 film deposited on the silicon substrate under the same deposition conditions, clearly indicates the formation of a mixed crystalline phase of anatase and rutile, with hexagonal symmetry and the following lattice parameters: a=b=0.38 nm and c=0.92 nm in the case of anatase and a=b=0.46 nm and c=0.29 nm in the case of rutile. The dominant phase of 78% is the rutile phase.

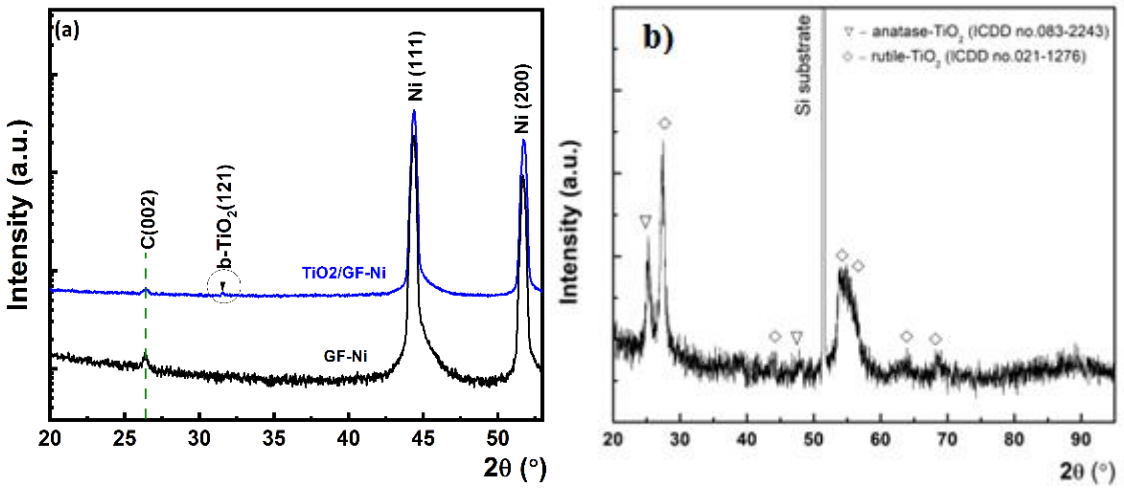

Fig. 3.3.2 X-ray diffraction spectra for (a) graphene grown by CVD on Ni foam (3D-GF/Ni, black line) and TiO_2^{RF}/3D –GF/Ni (blue line), (b) TiO_2 deposited on Si. Indexing was done using the ICDD database. [225]

The Raman spectra of TiO_2^{RF}/3D-GF/Ni nanomaterial shown in Fig 3.3.3, indicate the presence of a mixed rutile-anatase phase, with the characteristic peaks of TiO_2 anatase (147.5 cm^{-1}, 526.2 cm^{-1}) as well as TiO_2 rutile (445.2 cm^{-1}, 614.5 cm^{-1}). In addition, after TiO_2 film deposition on the 3D-GF/Ni structure, the position of G (1584.6 cm^{-1}), 2D (2684.2 cm^{-1}), and

D’ (1622.4 cm^{-1}), characteristic to the graphene, are identical to those before the TiO_2 deposition. Raman analysis indicates the achievement of a high-quality, defect-free graphene-based nanomaterial and suggests the presence of an anatase-rutile mixed phase in the case of TiO2 thin films.

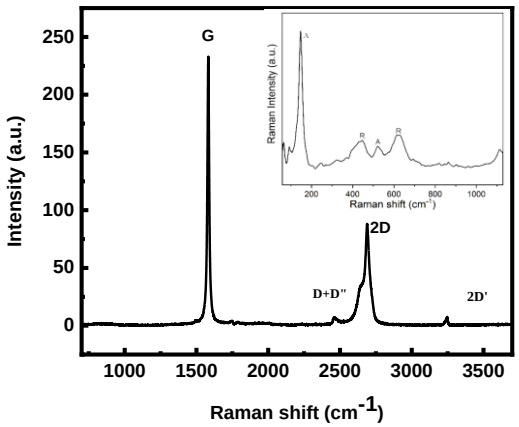

Fig. 3.3.3 Raman spectrum for the nanomaterial TiO_2^{RF}/3D –GF/Ni (A = anatase, R = rutile).

To evaluate the influence of the porous structure, as well as the reversibility of the process, the cyclic voltammetry profiles recorded at different scanning rates, from 20 to 200 mV/s, presented in Fig. 3.3.4, were performed.

In the inset, Fig. 3.3.4 shows the linear dependence of the current maximum with the square root of the scan rate, indicating the presence of a diffusion-controlled process.

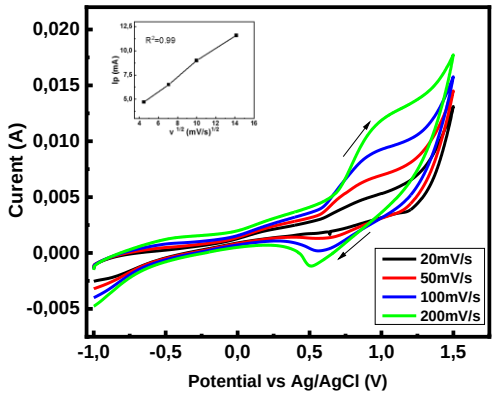

Fig. 3.3.4 CV curves recorded in 0.1 M Na_2SO_4 solution at different scan rates (insert: Ipa dependence with v 1/2 for TiO_2^{RF}/3D –GF/Ni hybrid nanomaterial)

Conclusions: The studied materials were synthesized by chemical vapor deposition in the case of graphene on nickel foam (3D-GF/Ni), and the hybrid TiO_2/3D-GF/Ni by titanium dioxide deposition employing sol-gel and RF Sputtering methods. Surface morphological characterizations showed that both graphene and TiO_2 film replicate the structure of Ni foam.

XRD and Raman's investigations suggest the presence of a mixed anatase-rutile phase structure for the TiO_2 thin films deposited by RF Sputtering and an anatase phase for the TiO_2 films obtained by the sol-gel method. Cyclic voltammetry indicated the electrochemical stability of the synthesized hybrid nanomaterial.

Chapter 4

Studies regarding the evaluation of the photocatalytic performance of graphene and TiO_2-based nanomaterials. Case study – photodegradation of methyl orange

This chapter presents the results obtained in the photodegradation processes of the methyl orange (MO) dye using 3D nanomaterials synthesized from three-dimensional graphene and TiO2. The titanium dioxide film was deposited by different methods, sol-gel, and RF sputtering, highlighting the main structural and morphological properties responsible for the photodegradation process of a highly resistant aromatic azo dye, methyl orange, both in the UV and visible range.

4.1 Materials and methods used in determining the photocatalytic performances of the obtained nanohybrid materials

Photodegradation tests for each component of the obtained hybrid materials, 3D graphene grown on nickel foam and those two hybrid nanomaterials TiO_2^{SG}/3D-GF/Ni and TiO_2^{RF}/3D-GF/Ni, were performed in both UV and visible range of the electromagnetic spectrum. The photocatalytic tests were carried out in a 10 ml solution of methyl orange (9.98 mg/L), using two types of UV irradiation sources, a UV source of 6W and a fixed wavelength (365 nm), as well as a Pen-Ray type source with mercury with primary emission at 254 nm and secondary emission at 180 nm. On the other hand, visible photocatalytic studies were conducted in the presence of a 100 mW/cm2 solar simulator. Irradiation of the methyl orange solution in the presence of the photocatalyst was realized until decolorization, 180 minutes in the case of UV and 90 minutes in the case of solar simulator.

To evaluate the efficiency of the photocatalyst, the following aspects were studied: dye stability under UV/visible irradiation (photolysis), dye adsorption on the nanomaterial surface, and photocatalytic dye degradation.

The photocatalytic efficiency was evaluated by colorimetric analysis of the residual dye concentration every 30 minutes of exposure to the light source, by the following equation:

$D = (A0-A1)/A0 * 100$ (equation 4.1)

Where D is the degradation efficiency, A0 and A1 are the methyl orange absorption in the initial solution and after exposure, respectively.

4.2 Studies regarding the determination of the photocatalytic activity of the binary nanomaterial 3D-GF15/Ni

The UV-vis spectra and the time profile of C/C0 for exposure to visible and UV light revealed the stability of the MO solution. Practically, no photolysis occurs, and the solution retains the initial concentration after 90 minutes of irradiation.

A good adsorption capacity has been observed in the presence of the 3D-GF15/Ni photocatalyst; the concentration decreased by 24% after 30 minutes of contact with the dye in the dark. The dye degradation efficiency after 90 min of irradiation was 88% and 89% when the irradiation source was sunlight and UV-365, respectively.

4.3. Studies regarding the determination of the photocatalytic activity of the TiO_2^{SG}/3D-GF/Ni nanomaterial

The studies carried out on the TiO_2^{SG}/3D-GF/Ni nanohybrid material aimed to determine the photocatalytic efficiencies of the anatase/graphene and to emphasize the influence of the quantity of titanium dioxide deposited and the solution pH on the photocatalytic efficiency degradation of the methyl orange.

Figure 4.3.1 shows the absorption spectra acquired after different periods of exposure to UV light and reveals the evolution of the azo chromophore at 504 nm with the increase of the exposure time to the UV light in the presence of the photocatalyst. The decrease in the intensity of the three absorption peaks at 504, 318, and 276 nm can be correlated with the azo bond and the pi-pi* transition in the aromatic rings of the dye and indicates the breaking of the azo bond of the chromophore. Concurrently, a new peak arises at 248 nm, which could be associated with the formation of byproducts in the degradation process of the dye.

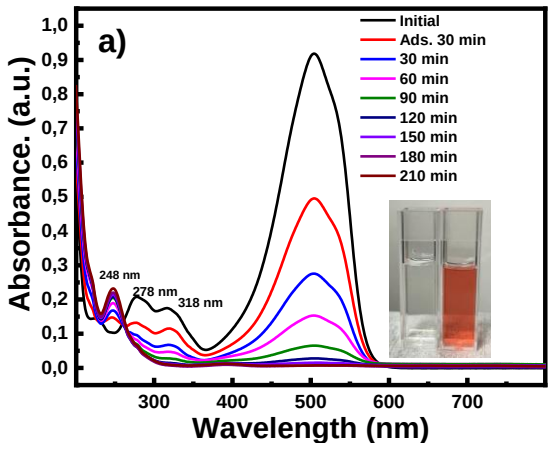

Fig. 4.3.1 Absorption spectra showing the photodegradation of methyl orange dye under UV irradiation in the presence of 4 cm^2 TiO_2^{SG}/3D-GF/Ni photocatalyst. Inset: photograph of the dye solution before (orange) and after 210 min (colorless) of UV exposure. [224]

As shown in the inset photo (Fig 4.3.1), after 210 minutes of exposure to UV-365 nm, the color of the solution changed from orange to colorless, indicating complete decolorization but incomplete degradation; in the solution, for sure, other molecules appeared that could not yet be identified.

Studies on samples with a geometric area of 1cm^2 and 4 cm^2 on which TiO_2 was deposited in identical conditions (4 cycles) have shown a strong influence of the surface on the photocatalytic process. In addition, high dye adsorption per unit volume is observed due to the large number of reactive centers created by increasing the geometric area to 4 cm2, further supporting the significant improvement of the degradation efficiency as more dye molecules are placed near the photocatalytic surface.

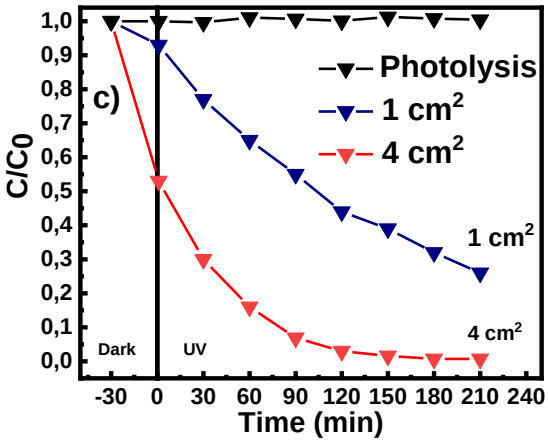

Fig 4.3.2 Influence of photocatalyst size synthesized in identical conditions on the photochemical decolorization of the methyl orange solution by exposure to the UV [224].

The photocatalytic study of TiO_2^{SG}/3D-GF/Ni was extended to the sunlight irradiation conditions. To emphasize the influence of the TiO_2 deposited quantity, two TiO_2^{SG}/3D-GF/Ni samples of 4 cm^2 and 1 cm^2, each coated by 3 and 4 deposition cycles of titanium dioxide, were tested under the same conditions of volume and concentration of methyl orange under light irradiation. In the case of 1 cm^2 samples, deposited amounts for 3 and 4 deposition cycles were 1.2 mg, and 1.6 mg, respectively. In the case of 4 cm2 samples, deposited amounts for 3 and 4 deposition cycles were 6 mg and 8 mg, respectively.

The time profile of C1/C0 under UV-365 nm and visible irradiation is shown in Fig 4.3.3, and data analysis indicates a significant mass influence in the case of 1 cm^2 samples, with an increase in degradation efficiency from 62% to 73% after 210 minutes of exposure to UV-365 nm (Fig. 4.3.3a). But, in the case of 4 cm^2 samples exposed to visible light, the efficiency of the MO degradation shows a similar behavior regardless of the deposition cycles, with the degradation efficiency above 99% after 90 minutes of irradiation (Fig 4.3.3b).

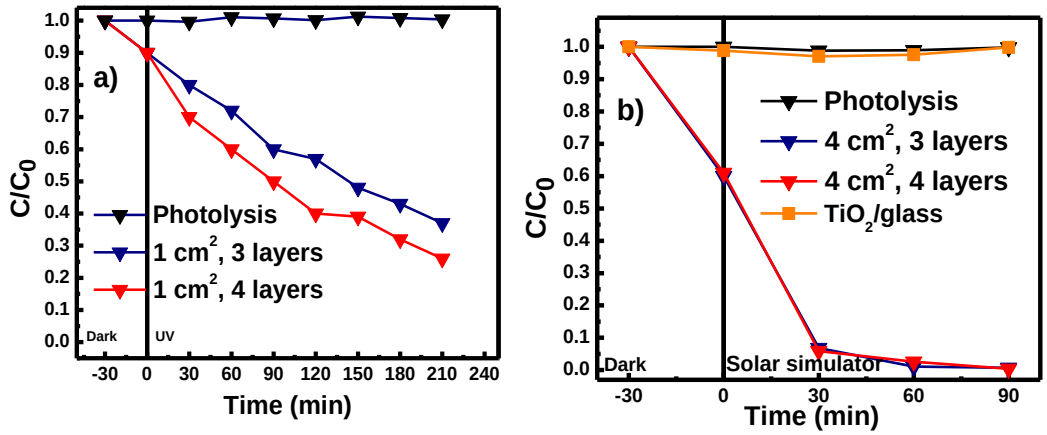

Fig. 4.3.3 Influence of TiO_2 amount per unit area on MO degradation in the presence of TiO_2^{SG}/3D-GF/Ni after exposure to a) UV and b) visible light [225].

The increase in photodegradation efficiency under simulated sunlight could, generally, be attributed to an increase in absorption in the visible range and/or efficient charge separation at the carbon-anatase interface.

In addition, the TiO_2^{SG}/3D-GF/Ni photocatalyst is robust and stable, allowing more cycles of sequential photodegradation and showing a similar efficiency after the third cycle in the case of the 4 cm^2 sample.

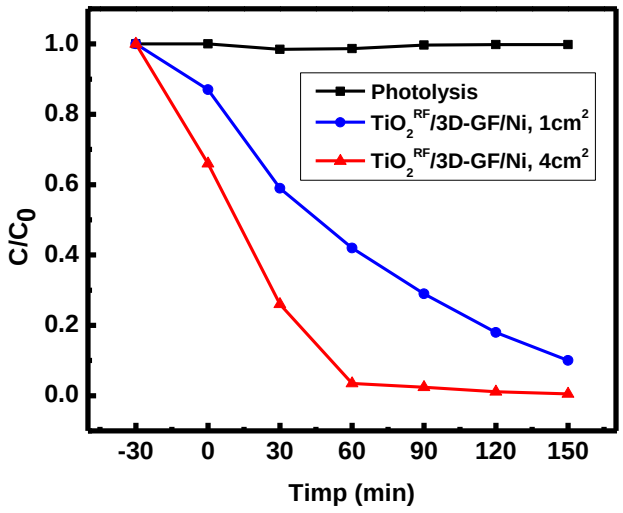

Fig.4.3.4 Studies on the photocatalytic efficiency of the rutile + anatase TiO_2^{RF}/3D-GF/Ni nanomaterial

The TiO_2^{RF}/3D-GF/Ni hybrid nanomaterial synthesized by the RF Sputtering method consisting of an anatase-rutile phase mixture, with the rutile predominant phase (78%), was evaluated from a photocatalytic point of view in the same case study on degradation of methyl orange.

Degradation tests of methyl orange as a function of irradiation time, UV-365 nm or solar simulator, for the nanomaterial of mixed rutile-anatase phase and geometric surfaces of 1 cm^2 and 4 cm^2 are shown in figure 4.3.4.

It is observed that the nanomaterial with a geometric surface of 1 cm^2 shows a degradation efficiency similar to the TiO_2^{RF}/3D-GF/Ni material with a geometric surface of 4cm^2 with the difference that the photocatalyst with an area of 4 cm^2 reaches the maximum decolorization after 180 minutes of UV irradiation, while for 1 cm^2 it takes 210 minutes to reach the same degradation efficiency (Fig 4.3.5a). In the case of exposure to simulated sunlight, the degradation efficiency reaches a value of 97.5 % after 90 minutes of irradiation, similar to the efficiency obtained under UV-365 nm irradiation after 180 minutes of exposure.

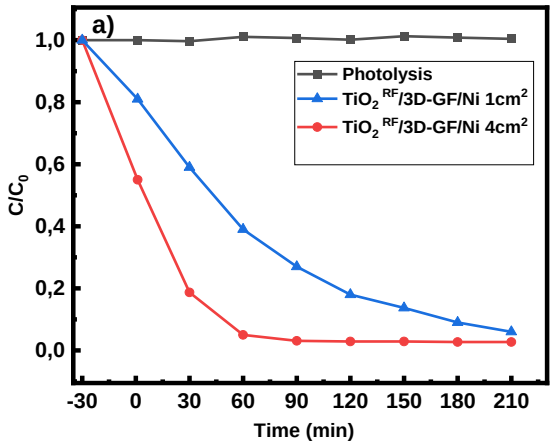

Fig. 4.3.5 Methyl orange degradation depending on a) UV and b) simulated sunlight irradiation for the TiO_2^{RF}/3D-GF/Ni nanomaterial with the geometric surfaces of 1 cm^2 and 4 cm^2

Repeatability tests also demonstrated retention of degradation efficiency after three cycles of use.

4.4 Studies on the degradation mechanism of methyl orange

The photocatalytic mechanism in nanomaterials based on hybrids of graphene with semiconductors is generally attributed to the heterojunctions formed by the two components and the generation of various reactive oxidative species (holes, hydroxyl and superoxide radicals). For the degradation processes to take place, the position of the conduction and valence bands relative to the redox potentials of the active species is important.

The conduction and valence bands of the nanomaterial with the anatase phase and band gap Eg = 3.07 eV are -0.23 eV and 2.84 eV, respectively.

In order to establish the main active species generated during the photocatalytic processes, a series of photodegradation experiments were carried out in the presence of scavengers. Ethylenediaminetetraacetic acid (EDTA), p-benzoquinone (BQ) and dimethyl sulfoxide (DMSO) or tert-butanol (tBuOH) were used as scavergers of holes (h+), superoxide radicals (•O2–) and hydroxyl radicals (•OH), respectively. The presence of active species in the photodegradation processes was determined by evaluating the variation over time of the C/C0

concentration after the addition of compounds that inhibit the generation of active species due to their affinity for those species. The results obtained for the TiO2SG/3D-GF/Ni hybrid under simulated sunlight exposure in the presence and absence of hole (EDTA), superoxide radicals (BQ), and hydroxyl radicals (DMSO) scavengers are shown in Figs. 4.4.1, and indicate a decrease in the degradation rate, suggesting that the oxidation processes of methyl orange are governed by holes with a smaller contribution of hydroxyl and superoxide radicals.

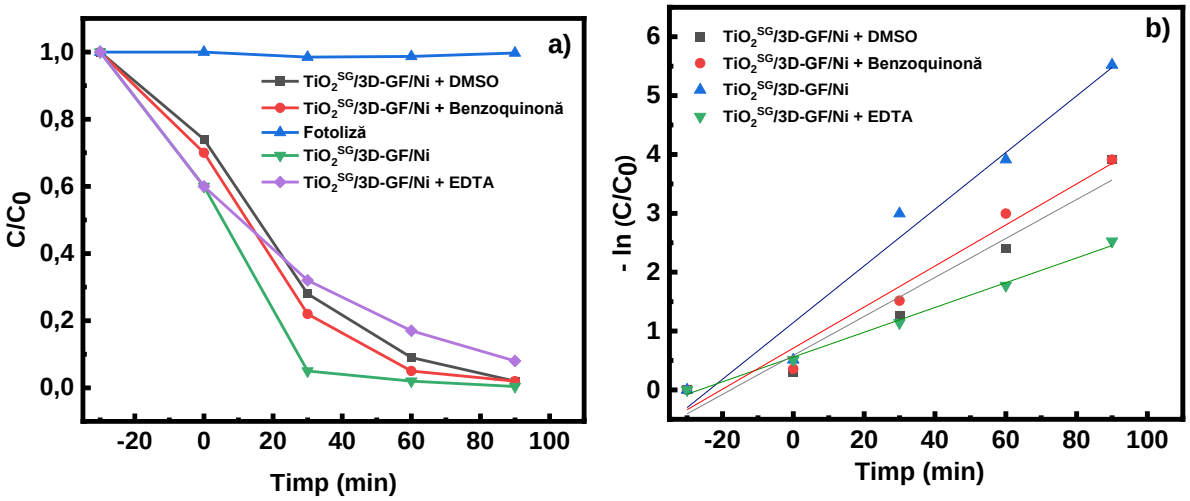

Fig.4.4.1 Photodegradation of methyl orange by TiO_2^{SG}/3D-GF/Ni in the presence of scavengers – holes-EDTA, superoxide radicals – BQ, and hydroxyl radicals – DMSO under simulated sunlight exposure.

Thus, the high photocatalytic activity observed in the TiO_2^{SG}/3D-GF/Ni hybrids could be a cumulative contribution due to the efficiency of the TiO_2/graphene interfaces, which hinder the electro-hole recombination, and, thus, more holes react with the H_2O or HO molecule to form hydroxyl radicals that increase the dye degradation process.

Conclusions - The systems of dye solutions and photocatalysts were subjected to the following experiments: (i) UV and simulated sunlight irradiation of the dye solution in the absence of the photocatalyst for 210 and 90 minutes, respectively, for photolysis studies; (ii) direct contact of the photocatalyst with the dye solution in the dark for 30 minutes, for adsorption studies; (iii) direct contact of the photocatalyst with the dye solution, and UV irradiation for 210 minutes, or simulated sunlight irradiation for 90 minutes to study the photodegradation process.

- The hybrid nanomaterials 3D-GF, TiO_2^{SG}/3D-GF/Ni, and TiO_2^{RF}/3D-GF/Ni showed to be efficient for methyl orange degradation under both UV and simulated sunlight irradiation.

- The photocatalysis study emphasized the influence of some parameters that influence the efficiency of the photodegradation process: the geometric surface of the photocatalyst to solution volume ratio, the amount of dye-graphene and TiO^2/cm^2 of material, and solution pH.

- For an adequate photocatalyst-dye solution ratio cm^2.mL, of at least 1/10, the degradation efficiency is greater than 90% after 30 minutes of sunlight exposure and 90 minutes of UV light exposure, making the TiO_2^{SG}/3D-GF/Ni hybrid one of the most efficient photocatalysts with visible activity for degradation of an azo dye, methyl orange.

- The degradation efficiency for TiO_2^{SG}/3D-GF/Ni and TiO_2^{RF}/3D-GF/Ni nanomaterials of 99.5% and 97.5%, respectively, recorded at 90 minutes of sunlight irradiation exceeds the performances reported thus far for photocatalysts immobilized on different substrates. [198-212]

- The main oxidative species involved in the photodegradation process of methyl orange were holes and, to a lesser extent, hydroxyl, and superoxide radicals.

Chapter 5

Conclusions, original contributions and perspectives

5.1 Conclusions

In this doctoral thesis entitled "Development of new hybrid nanomaterials based on 3D graphene and TiO2 for the degradation of pollutants in industrial waters", hybrid photocatalytic systems based on titanium dioxide and three-dimensional graphene for the degradation of persistent pollutants from waters have been synthesized and characterized. The role of the obtained hybrid nanomaterials is to serve as a photocatalyst in the purification of waters contaminated with dyes from the textile industry. Their photocatalytic performances were tested in the presence of a synthetic dye (MO) under both UV and simulated sunlight irradiation.

Literature studies on the photocatalytic activity of nanomaterials highlight the existence of numerous nanomaterials that have been explored as photo- and electro-catalysts. The most studied are titanium dioxide or several other metallic oxides, and recently graphitic carbon nitride (g-C3N4), graphene, and its derivatives have gained significant attention in the photocatalytic field.

Graphene has a unique two-dimensional structure with a large surface area, high conductivity, and electron mobility, which makes it capable of effectively reducing electron-hole pair recombination and thus improving photocatalytic efficiency.

Although titanium dioxide particles have a higher dye degradation efficiency than titanium dioxide films due to their large surface area, they present a high disadvantage, namely that of recovery difficulty from an aqueous medium and reusability, which require advanced technologies that are very expensive.

Starting from three-dimensional graphene synthesized by the CVD method on nickel foam as support, titanium dioxide - 3D graphene hybrids were synthesized. Two methods were employed to obtain the hybrids, one is a top-down approach, such as RF sputtering, and the other, is a bottom-up type, such as the sol-gel method. The titanium dioxide deposited by the RF Sputtering process formed a uniform and continuous film over the entire graphene surface, but in a mixed rutile and anatase phase, according to XRD and Raman investigations, resulting in the nanomaterial denoted TiO2RF/3D-GF/Ni.

On the other hand, the sol-gel method led to the synthesis of single-phase anatase thin films based on the XRD and Raman analysis, resulting in the nanomaterial denoted TiO2SG/3D-GF/Ni.

For the morpho-structural characterization, morphology and elemental composition analyses were performed by scanning electron microscopy (SEM). X-ray diffraction (XRD) and Raman spectroscopy measurements were performed to determine the phase. The electrochemical characterization of the 3D-GF/Ni, TiO2SG/3D-GF/Ni, and TiO2RF/3D-GF/Ni structures was performed through cyclic voltammetry tests.

The analysis of morphology and composition indicated that in the case of both hybrid materials, the one obtained by sol-gel method and the one obtained by RF Sputtering method, the graphene layer is completely covered with the TiO_2 thin film which, however, shows small cracks, thus resulting the innovative TiO2/3D-GF/Ni hybrid material. In addition, the surface morphological characterizations show that even after the deposition of the TiO_2 thin film, the sample retains its porous structure, with both the graphene layer and the TiO_2 film replicating the structure of the Ni foam.

Cyclic voltammetry was used to characterize the electrochemical stability of the synthesized hybrid material; no redox reactions involving the material were detected. Both obtained materials showed electrochemical stability, recording up to 50 cycles with the same shape, some even identical. The material deposited by RF Sputtering, which presents a combination of the anatase and rutile phases, and the material deposited by the sol-gel method, which presents only the anatase phase, showed an oxidation maximum in the cyclic voltammogram recorded in a solution of 50 mg L^{-1} MO in 0.1 M Na_2SO_4 electrolyte around 0.36 V and 0.450 V, respectively.

The photocatalytic activity of the hybrid nanomaterials was validated under both UV and simulated sunlight illumination systems, at an irradiation power of 6W and 100 mW/cm2, respectively.

The use of nanomaterials, 3D-GF/Ni, TiO_2^{SG}/3D-GF/Ni, and TiO_2^{RF}/3D-GF/Ni in the photochemical degradation of persistent organic pollutants, specifically methyl orange dye, showed a degradation efficiency of each material under both the visible and UV range. Within

the photodegradation process, the contribution of each process was studied, namely adsorption and photodegradation in the presence and absence of the photocatalyst.

The systems formed from the dye solutions and the photosensitive catalysts were tested through the following stages: (i) photolysis of the methyl orange solution - UV and simulated sunlight irradiation for 210/90 minutes; (ii) adsorption in the dark - direct contact with the photocatalyst material for 30 minutes to ensure the adsorption-desorption equilibrium, (iii) photodegradation - direct contact with the photocatalyst material and UV and visible irradiation, until decolorization for 210 and 90 minutes, respectively.

For a suitable photocatalyst-to-dye ratio (8 mg TiO2 – 10mg/L), the degradation efficiency is greater than 90% after 30 min exposure to the solar simulator and 90 min of UV exposure, making TiO2SG/3D-GF /Ni one of the most efficient sunlight-activated photocatalysts to decolorize the azo dye, methyl orange. It should also be mentioned the contribution that the 3D-GF/Ni material brings, primarily through the adsorption efficiency, which proved to be 42% after only 30 minutes of contact with the solution in the dark.

After 180 minutes of exposure to UV-365 nm, the TiO_2^{SG}/3D-GF/Ni hybrid nanomaterial recorded the highest degradation efficiency of 99%, and the TiO_2^{RF}/3D-GF/Ni nanomaterial a degradation efficiency of 97.3% and 97, 2 % in the case of 3D-GF/Ni. In the case of exposure to the solar simulator, the degradation efficiency after only 90 minutes for TiO_2^{SG}/3D-GF/Ni and TiO_2^{RF}/3D-GF/Ni was 99.5% and 97.5%, respectively.

The higher degradation efficiency in the case of the TiO2SG/3D-GF/Ni nanomaterial can be justified based on the effect induced by the mass/polymorphism of the titanium dioxide. For instance, the amount of TiO2 deposited by this method is higher (8 mg) than by the RF Sputtering approach (6mg), and the pure anatase phase in the first case but a mixture of rutile (78%) and anatase (22%) in the second case.

After 3 cycles of reuse of the two nanomaterials, TiO_2^{SG}/3D-GF/Ni and TiO_2^{RF}/3D-GF/Ni with a geometric surface of 4cm^2, they demonstrated a degradation efficiency similar to that of the first cycle, which proves that they have a good regeneration capacity, with the preservation of photocatalytic properties after 270 minutes of exposure to the solar simulator.

5.2 Original Contributions

To depict the original contributions, several research activities were considered that helped in the synthesis, characterization, and testing of nanomaterials obtained based on 3D graphene and TiO2. Among them, the following are presented:

 Preparing a study as complex as possible in the specialist literature regarding hybrid nanomaterials, aiming to present some original elements in the scientific approach to obtaining hybrid nanomaterials based on 3D graphene and TiO2 film used in water remediation.

 Carrying out preliminary tests in which process parameters were varied, on different substrates (FTO, Si, quartz) in order to identify the optimal parameters for obtaining the 3D graphene structure - TiO_2 and characteristics of metallic oxide; TiO_2 was deposited on Si by

RF sputtering to determine the thickness of the deposited film, and on quartz to determine the band gap.

 The design and synthesis of hybrid nanomaterials of the last generation, in which the active material is immobilized on the substrate, with excellent photocatalytic properties in the visible range of the electromagnetic spectrum, due to the three-dimensional structure and the interfaces created between graphene and titanium dioxide.

 Development of a conceptual research model that materialized in synthesis methods for each component of the hybrid structures as well as morphological and electrochemical characterizations: morpho-structural characterization by scanning electron microscopy (SEM), determination of phase, structure, and purity by X-ray and Raman spectroscopy, determination of elemental composition by energy dispersive X-ray spectroscopy (EDS), and testing of electrochemical properties by cyclic voltammetry.

 The study of photocatalytic properties in the presence of a dye frequently used in the textile industry and very resistant to degradation processes, methyl orange.

 Elaboration of a work plan regarding the laboratory experiments in order to establish the optimal working parameters specific to the dye degradation process. In this sense, a complex, rational work plan was elaborated, a plan that was followed with perseverance.

 The optimal material variants have chosen, and the MO oxidation parameters were subsequently studied (concentration, pH, UV wavelength) to ensure a quasi-total degradation of MO.

 The importance of the synthesis method to obtain the anatase phase with the best performance in the presence of visible radiation of the electromagnetic spectrum.

 Testing and validating the photocatalytic performances of 3D-GF/Ni, TiO_2^{SG}/3D-GF/Ni, and TiO_2^{RF}/3D-GF/Ni nanomaterials and establishing the degradation mechanism of methyl orange.

5.3 Prospects

- Evaluation of photocatalytic performances for other dyes, including persistent organic pollutants.

- Continuation of tests in order to establish the degradation mechanism of methyl orange for both materials.

- Determination of the specific surface area of the synthesized nanomaterials

- Pilot-scale design of a remediation reactor in continuous mode using photocatalytic nanomaterials.

BIBLIOGRAPHY

[1] Recommendation on the Definition of Nanomaterial, European Commission, Brussels, Belgium 2011, https://eur-lex.europa.eu/ legal-content/EN/TXT/?uri=CELEX:32011H0696 (accessed: May 2019).

[2] D. V. Talapin, E. V. Shevchenko, Chem. Rev. 2016, 116, 10343.

[3] R. Kodama, J. Magn. Magn. Mater. 1999, 200, 359.

[4] H. Kim, R. P. Carney, J. Reguera, Q. K. Ong, X. Liu, F. Stellacci, Adv. Mater. 2012, 24, 3857.

[5] A. Cirri, A. Silakov, B. J. Lear, Angew. Chem., Int. Ed. 2015, 54, 11750.

[6] M. Reza Nejadnik, W. Jiskoot, J. Pharm. Sci. 2015, 104, 698.

[7] C. Gong, M. R. S. Dias, G. C. Wessler, J. A. Taillon, L. G. SalamancaRiba, M. S. Leite, Adv. Opt. Mater. 2017, 5, 1600568.

[8] Savage, N. & Diallo, M. S. Nanomaterials and Water Purification: Opportunities and Challenges. Journal of Nanoparticle Research 7, 331–342 (2005).

[9] Ihsanullah, I. MXenes (two-dimensional metal carbides) as emerging nanomaterials for water purification: Progress, challenges, and prospects. Chemical Engineering Journal 388, 124340 (2020).

[10] Keshav K. Singh, Role of Nanotechnology and Nanomaterials for Water Treatment and Environmental Remediation, International Journal of New Chemistry (2020)

[11] Das, R. et al. Recent advances in nanomaterials for water protection and monitoring. Chemical Society Reviews (2017).

[12] Ibhadon, A.O.; Fitzpatrick, P. Heterogeneous photocatalysis: Recent advances and applications. Catalysts 2013, 3, 189–218

[13] Wei, W.; Liu, D.; Wei, Z.; Zhu, Y. Short-range π-π stacking assembly on P25 TiO2 nanoparticle for enhanced visible-light photocatalysis. ACS Catal. 2017, 7, 652–663.

[14] Jiang, W.J.; Liu, Y.F.; Wang, J.; Zhang, M.; Luo, W.J.; Zhu, Y.F. Separation-free polyaniline/TiO2 3D hydrogel with high photocatalytic activity. Adv. Mater. Interfaces 2016, 3, 9.

[15] Tatsuma,T.;Saitoh,S.;Ohko,Y.;Fujishima,A.TiO2-WO3 photoelectrochemical anticorrosion system with an energy storage ability. Chem. Mater. 2001, 13, 2838–2842.

[16] Sajan, C.P.; Wageh, S.; Al-Ghamdi, A.A.; Yu, J.G.; Cao, S.W. TiO2 nanosheets with exposed {001} facets for photocatalytic applications. Nano Res. 2016, 9, 3–27.
[17] Chen, X.; Mao, S.S. Titanium dioxide nanomaterials: Synthesis, properties, modifications, and applications. Chem. Rev. 2007, 107, 2891–2959.
[18] Tong, H.; Ouyang, S.X.; Bi, Y.P.; Umezawa, N.; Oshikiri, M.; Ye, J.H. Nano-photocatalytic materials: Possibilities and challenges. Adv. Mater. 2012, 24, 229–251.
[19] Anpo, M.; Tackeuchi, M. The design and development of highly reactive titanium oxide photocatalysts operating under visible light irradiation. J. Catal. 2003, 216, 505–516.
[20] Al-Harbi, L.M.; El-Mossalamy, E.H.; Arafa, H.M.; Al-Owais, A.; Shah, M.A. TiO2 Nanoparticles with Tetra-pad Shape Prepared by an Economical and Safe Route at very Low Temperature. Mod. Appl. Sci. 2011, 5, 130–135.
[21]Giovannetti,R.;D'Amato,C.A.;Zannotti,M.;Rommozzi,E.;Gunnella,R.;Minicucci,M.;DiCicco,A.Visible light photoactivity of polypropylene coated nano-TiO2 for dyes degradation in water. Sci. Rep. 2015, 2.
[22] Mills, A.; Le Hunte, S. An overview of semiconductor photocatalysis. J. Photochem. Photobiol. A 1997, 108, 1–35.

Dissemination of results

Articole publicate in reviste cotate Web of Science in domeniul tezei de doctorat

1.**Elena Madalina Mihai**, Iuliana Mihalache, Anca-Ionela Istrate, Cristina Banciu, Cosmin Romanitan, Oana Brancoveanu, Eugenia Tanasa, Alexandra Banu, Lucia Monica Veca , Self-Sustained Three-Dimensional Macroporous TiO_2-Graphene Photocatalyst for Sunlight Decolorization of Methyl Orange, Nanomaterials, 12, 4393, 2022, IF: 5,719 https://doi.org/10.3390/nano12244393

Articole publicate in reviste indexate Web of Science in domeniul tezei de doctorat

2. **Elena Madalina Mihai**, Anca-Ionela Istrate, Octavian Gabriel Simionescu, Cristina Banciu, Cosmin Romanitan, Florin Comanescu, Alexandra Banu, L.Monica Veca, Synthesis of TiO_2/GF-Ni hybrid materils by a combined chemical vapor deposition/ RF Magnetron Sputtering approach, U.P.B. Sci. Bull., Series B, Vol. 83, Iss. 4, 2021, ISSN 1454-2331

3.Alexandra Banu, **Madalina Mocirla**, Gizem Nur Soylu, Preliminary study of electrochemical advanced oxidation of organic dyes on TiO_2, MATEC Web of Conferences **299**, 01002 (2019) *MTeM 2019,* https://doi.org/10.1051/matecconf/201929901002

4. Luciana Laura Dincă (Shamieh) Alexandra Banu, Gizem Nur Soylu, Gabriel Dobri and **Madalina Elena Mocirla (Mihai)**, The effects of growth TiO_2 nanotubes on forged TI6AL4V alloyand selective laser sintered TI6AL4V alloy surfaces for environmental and medical applications, MATEC Web of Conferences **299**, 01005 (2019), *MTeM 2019,* https://doi.org/10.1051/matecconf/201929901005